Available online at www.sciencedirect.com

SCIENCE DIRECT®

Journal of Nuclear Materials 326 (2004) 106–113

journal of nuclear materials

www.elsevier.com/locate/jnucmat

Production behavior of irradiation defects in α-alumina and sapphire under ion beam irradiation

Kimikazu Moritani, Ikuji Takagi, Hirotake Moriyama *

Department of Nuclear Engineering, Graduate School of Engineering, Kyoto University, Yoshida-honmachi, Sakyo-ku, Kyoto 606-8501, Japan

Received 1 April 2003; accepted 28 December 2003

Abstract

The production behavior of irradiation defects in α-alumina and sapphire was studied by in situ luminescence measurement technique under ion beam irradiation of H^+ and He^+. The luminescence intensity of the F^+ centers at 330 nm was observed to decrease monotonically with the increasing temperature up to 800 K, while the intensity of the F^0 centers at 410 nm to show non-monotonic temperature dependence. In the latter case, the intensity decreased with the temperature up to 600 K, and then increased above this temperature. It was also observed that the luminescence intensity at 410 nm was lower in the He^+ irradiation than in the H^+ irradiation. These observations wereanalyzed by considering the production mechanisms and reaction kinetics of the irradiation defects of F-type centers.

1. Introduction

Irradiation behavior of ceramic materials is one of the topics of current interest, since some of these materials are to be used in the strong radiation field of proposed fusion reactors. However, the dynamic production behavior of irradiation defects under irradiation has not been fully clarified in spite of the considerable progress in understanding many aspects of irradiation defects in these ceramic materials. It is thus important to know the production behavior of irradiation defects by such an in situ luminescence measurement technique.

For fusion reactor blanket materials, we have already studied the production behavior of irradiation defects in some candidate lithium ceramics by an in situ luminescence measurement technique under ion beam irradiation [1]. In Li_2O, it has been confirmed that the F^+ center (an oxygen vacancy trapping an electron) and the F^0 center (an oxygen vacancy trapping two electrons), which are commonly observed in ionic compounds, are formed by irradiation [2,3]. Similar irradiation defects of F-type centers are also produced in $LiAlO_2$ [4], Li_2TiO_3, Li_2ZrO_3 and Li_2SnO_3 [5,6]. These defects are considered to play an important role in the tritium behavior [1].

Following the measurement of lithium ceramics, the present study deals with α-alumina and sapphire in which the F-type centers are produced [7–11]. These ceramics are often used as refractory oxide dielectric materials in the radiation field, it is also needed to know the dynamic behavior of the irradiation defects. In the present study, similarly to the case of lithium ceramics, the luminescence spectra were measured under ion beam irradiation, and the temperature dependence of the luminescence intensity was analyzed by considering the production mechanism and reaction kinetics of the irradiation defects.

---

* Corresponding author. Tel./fax: +81-75 753 5824.

E-mail address: moriyama@nucleng.kyoto-u.ac.jp (H. Moriyama).

0022-3115/$ - see front matter © 2004 Elsevier B.V. All rights reserved.
doi:10.1016/j.jnucmat.2003.12.010

2. Experimental

The pellet-type specimen of α-alumina and sapphire was obtained from Kyocera Co. Ltd., which was of 10 mm in diameter and about 0.5 mm in thickness, and was irradiated with H^+ and He^+ ion beam, accelerated to 2 MeV with a Van de Graaff accelerator. The size of the ion beam was about 3 mm × 3 mm and its current was monitored. The luminescence from the target sample was led to monochromaters, Ritsu MC-20N, and counted with photo-multipliers, Hamamatsu R585. A photonic multichannel analyzer, Hamamatsu PMA-11 was also used to measure the irradiation time dependence of the luminescence. The temperature of the sample holder was controlled with an electric heater and a thermocouple while another thermocouple was attached to the sample surface to monitor its temperature. The experimental conditions are summarized in Table 1.

Table 1
Experimental conditions

Specimen	Irradiation condition		
	Projectile	Beam current (nA/cm^2)	Temperature (K)
α-Alumina	2 MeV H^+	10–240	302–904
	2 MeV He^+	10–900	300–799
Sapphire	2 MeV H^+	20–150	298–824
	2 MeV He^+	120–900	307–789

3. Results and discussion

3.1. Luminescence bands

Fig. 1 shows typical luminescence spectra of α-alumina under He^+ ion beam irradiation and Fig. 2 shows those of sapphire under H^+ irradiation. For comparison, the ordinate represents luminescence intensity normalized to the beam current of 10 nA/cm^2; the peak heights have been observed to be proportional to the beam current and then all of the spectra in the present study are corrected with the beam current. Similar spectra were also observed for other cases. As shown in Fig. 1, the observed luminescence spectra are decomposed into a number of luminescence bands, namely 330, 420 nm and others. For the decomposition, following the manner in the previous study [5], energy-based Gaussian functions were taken for all the luminescence bands and the peak heights and positions were determined.

In the case of α-alumina and sapphire, there have been reported a number of F-type centers including the F^+ and F^0 centers [7]. As for the luminescence of irradiation defects, it is known that the luminescence of the F^+ center is observed at the UV region around 3.8 eV (325 nm) while that of the F^0 centers is observed at a lower photon energy region around 3.0 eV (410 nm). Thus the presently observed luminescence from α-alumina and sapphire which is centered at 330 and 420 nm can be attributed to the F^+ and F^0 centers. As for the others, it is noted that the luminescence at 250 and 290 nm is also observed in the case of α-alumina. The luminescence intensity at these bands was found to be sensitive to thermal annealing at higher temperatures, and then might be attributed to the effect of some impurities such as OH. It was also found that the effect is more clearly observed in the case of H^+ irradiation. This may be explained by considering the local reactions of irradiation defects in the ion tracks. Specific ionization and hence the local concentration of irradiation defects are lower for H^+ than for He^+ and are much affected by such impurities.

3.2. Irradiation time dependence

As shown in Fig. 3, in the present experiment, it has been observed that the luminescence intensities at 330 and 420 nm show an irradiation history in which the intensities increase with irradiation time and reach the steady-state ones. By annealing the irradiated specimens above 1073 K for some tens minutes, such an irradiation history has been observed repeatedly. This fact suggests that a considerable part of the luminescence comes from the defects accumulated by irradiation and that the intensities at these bands may reflect the amounts of the F^+ and F^0 centers. A similar irradiation history has also been reported by Al Ghamdi and Townsend [8], who have measured the ion beam induced luminescence of sapphire. In their case, however, they have observed non-zero values for the luminescence intensity at a low fluence, and have suggested that the luminescence is from intrinsic color centers activated by excited electrons. In the present case, on the other hand, nearly zero values have been observed with annealed specimens and it follows that the luminescence originates from the F^+ and F^0 centers accumulated by irradiation.

In their experiment with electron irradiated sapphire [9], Morono and Hodgson have found that the peak height ratio between the F^+ and F^0 is strongly dependent on the dose rate and that the F^+ luminescence increases with the dose rate while the F^0 luminescence decreases. Since the F^+ is hardly accumulated in the electron irradiated sapphire, this dose rate effect has been explained by considering the conversion of the F^0 to the F^+; the F^0 is excited by electron and hole capture and this excited F^0 is ionized by hole capture giving the F^+ [9]. In the present case, on contrast, such a dose rate effect was hardly observed in the studied region, possibly due to low dose rates compared with the above case. Thus the presently observed luminescence intensities at 330 and 420 nm are considered to represent the accumulated F^+ and F^0 centers, respectively.

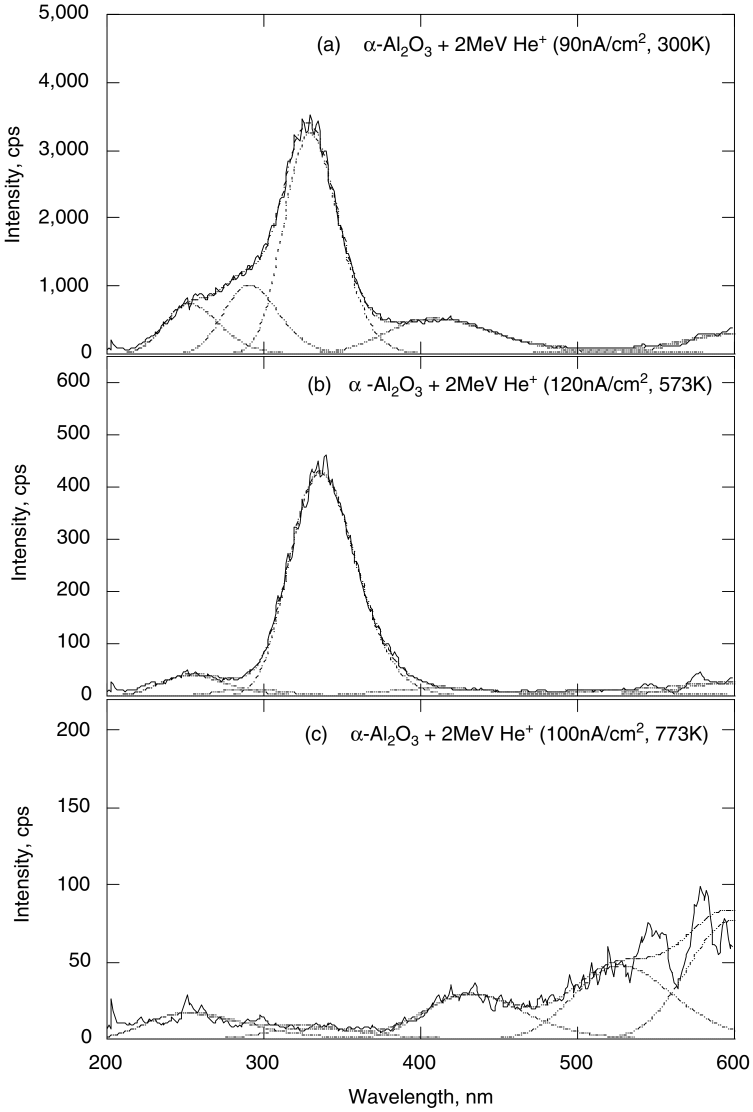

Fig. 1. Typical luminescence spectra of α-alumina under 2 MeV He$^+$ ion beam irradiation. The ordinate represents luminescence intensity normalized to the beam current of 10 nA/cm^2. Curves represent the results of decomposition as described in Section 3.1.

3.3. Temperature dependence

Fig. 4(a) and (b) show the Arrhenius plots of the steady-state luminescence intensity of α-alumina under H$^+$ and He$^+$ irradiation, respectively. Similarly, Fig. 5(a) and (b) show the luminescence intensity of sapphire under H$^+$ and He$^+$ irradiation, respectively. As shown in these figures, the intensity at 330 nm decreases monotonically with the increasing temperature up to 800 K. It seems to show that recombination proceeds at higher temperatures. In the case of the 420 nm luminescence, on the other hand, some non-monotonic temperature dependence can be seen; the intensity decreased with the temperature up to 600 K, and then increased above this temperature. In this case, not only recombination but also some additional production of the F^0 centers seem to be involved in the reaction scheme.

3.4. Production mechanism of irradiation defects

In the case of ionic compounds such as alumina, it is considered that the formation of such F-type defect centers of the F$^+$ and F^0 is accompanied with the formation of the interstitial O$^-$ and O^0, respectively. In addition to these, the O_2^- and O_2 may be formed by the reactions of $O^- + O^0 \rightarrow O_2^-$ and $O^0 + O^0 \rightarrow O_2$, although

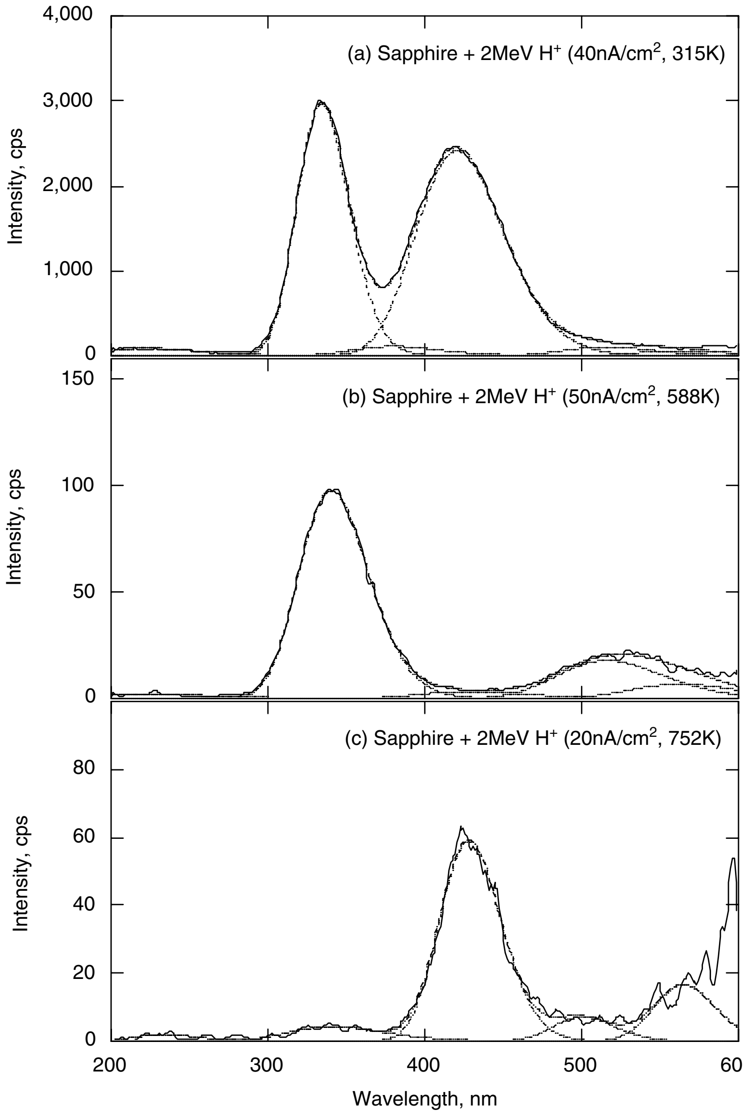

Fig. 2. Typical luminescence spectra of sapphire under 2 MeV H^+ ion beam irradiation. The ordinate represents luminescence intensity normalized to the beam current of 10 nA/cm^2. Curves represent the results of decomposition as described in Section 3.1.

the diffusion of the O_2^- and O_2 will be much slower than the O^- and O^0. Thus the following production mechanism of irradiation defects in α-alumina and sapphire can be suggested:

$$Al_2O_3 \rightarrow Al_2O_3^* \rightarrow F^+, F^0 \qquad (0)$$

$$F^+ + O^- \rightarrow \text{recombination (at lower temperatures)} \qquad (1)$$

$$F^+ + O_2^- \rightarrow \text{recombination (at higher temperatures)} \qquad (2)$$

$$F^+ + O_2^- \rightarrow F^0 + O_2 \quad \text{(additional } F^0 \text{ production at higher temperatures)} \qquad (3)$$

$$F^0 + O^0 \rightarrow \text{recombination (at lower temperatures)} \qquad (4)$$

$$F^0 + O_2 \rightarrow \text{recombination (at higher temperatures)} \qquad (5)$$

Reaction (0) represents the production of an excited Al_2O_3 ($Al_2O_3^*$) by ion beam irradiation, which is

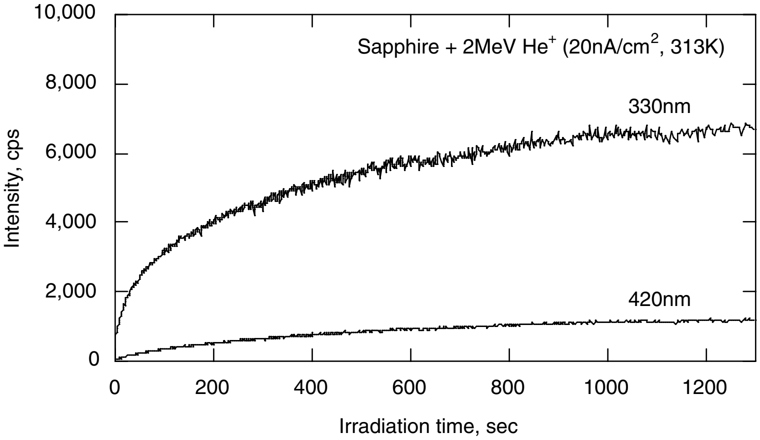

Fig. 3. Irradiation time dependence of the luminescence from sapphire under 2 MeV He^+ irradiation at 313 K. The specimen was annealed above 1073 K for 10 min.

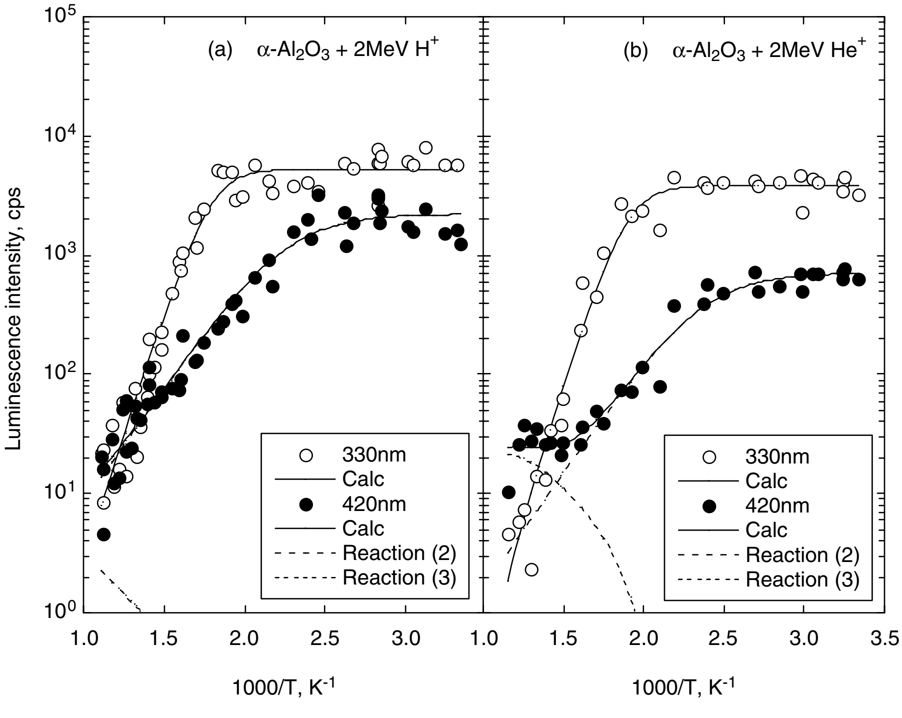

Fig. 4. Arrhenius plots of luminescence intensity of α-alumina under (a) 2 MeV H^+ and (b) 2 MeV He^+ irradiation. The ordinate represents luminescence intensity normalized to the beam current of 10 nA/cm^2. Marks are experimental and curves represent the least-squares fits of the data to Eqs. (10) and (11) as described in Section 3.5. Contributions of reactions (2) and (3) are also shown.

de-excited to F^+ and F^0. Reactions (1) and (2) represent the recombination of the F^+ with the O^- and O_2^-, respectively, while reaction (3) is to account for the additional production of the F^0 in the higher temperature region. Because of its larger size, the O_2^- is considered to be more responsible for reaction (3) in the higher temperature region than the O^-. Similarly to the case of the F^+, reactions (4) and (5) represent the recombination of the F^0 with the O^0 and O_2, respectively. All the reactions (1)–(5) are the second-order, but are treated as the first-order of the F^+ or F^0 in the following analysis for simplicity. In fact, for example, such an F^+ center is considered to be associated with an O^- interstitial under Coulomb interaction in the form of $(F^+{\cdot}O^-)$ as

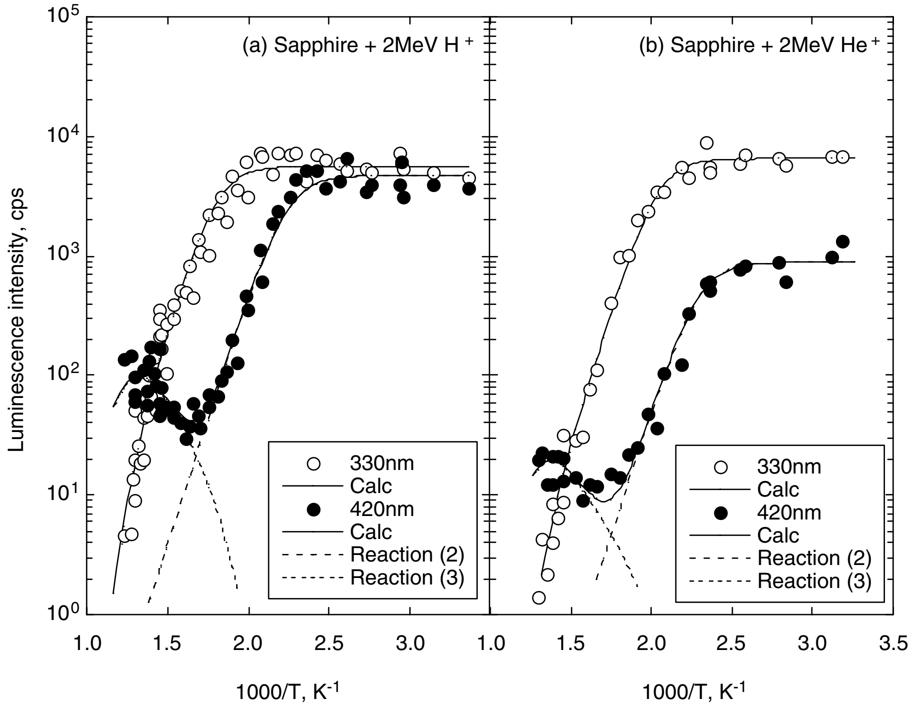

Fig. 5. Arrhenius plots of luminescence intensity of sapphire under (a) 2 MeV H^+ and (b) 2 MeV He^+ irradiation. The ordinate represents luminescence intensity normalized to the beam current of 10 nA/cm^2. Marks are experimental and curves represent the least-squares fits of the data to Eqs. (10) and (11) as described in Section 3.5. Contributions of reactions (2) and (3) are also shown.

suggested for Li_2O [2,3], and its reaction may be treated as the first-order.

3.5. Determination of kinetic parameters

It is interesting and important to obtain the rate constants of reactions involved in the production of irradiation defects. Based on the suggested reaction scheme, the observed temperature dependence of the luminescence intensity is analyzed here.

According to the literature [7], the luminescence at 3.8 eV (325 nm) is attributed to the singlet (2P to 1S*) emissions of the F^+ centers and 3.0 eV (410 nm) the triplet (^{3}P to ^{3}S*) of the F^0 centers, as shown in Fig. 6. Since the luminescence is caused from the F^+ and F^0 activated by excited electrons, the observed luminescence intensities I_{330} and I_{420} at 330 nm and 420 nm are proportional to the state densities of $[F^+(1A)]$ and $[F^0(^1S)]$, as given by

$$I_{330} = c_{F^+}[F^+(1A)], \tag{6}$$

$$I_{420} = c_{F^0}[F^0(^1S)], \tag{7}$$

where c_{F^+} and c_{F^0} are constants. The steady-state luminescence intensities have been measured in the present experiment, and then a steady-state approximation is applied to these states, that is

$$d[F^+]/dt = g_{F^+} - k_1[F^+] - k_2[F^+] - k_3[F^+] = 0, \tag{8}$$

$$d[F^0]/dt = g_{F^0} + k_3[F^+] - k_4[F^0] - k_5[F^0] = 0, \tag{9}$$

where g_{F^+} and g_{F^0} are the generation rate of F^+ and F^0 by reaction (0).

For the analysis of the observed temperature dependence of the luminescence intensity, Eqs. (8) and (9) are solved to obtain the steady-state densities of the F^+ and F^0 which are substituted into Eqs. (6) and (7). The rate constants are assumed to be of the Arrhenius type, and hence the pre-exponential term A_i and activation energy term E_i are determined in the analysis. Since the number of the parameters is so large and some of those are not independent, further assumptions are made for a proper convergence. By considering that the energy needed for the defect production and the defect reactions are essentially the same in the same specimen, the activation energy is assumed to be the same irrespective of the different projectile ions, H^+ or He^+ Also, the activation energy values for reactions (1) and (4) which are considered to be low are assumed to be zero, that is $E_1 = 0$ and $E_4 = 0$. As shown in Figs. 4 and 5, in

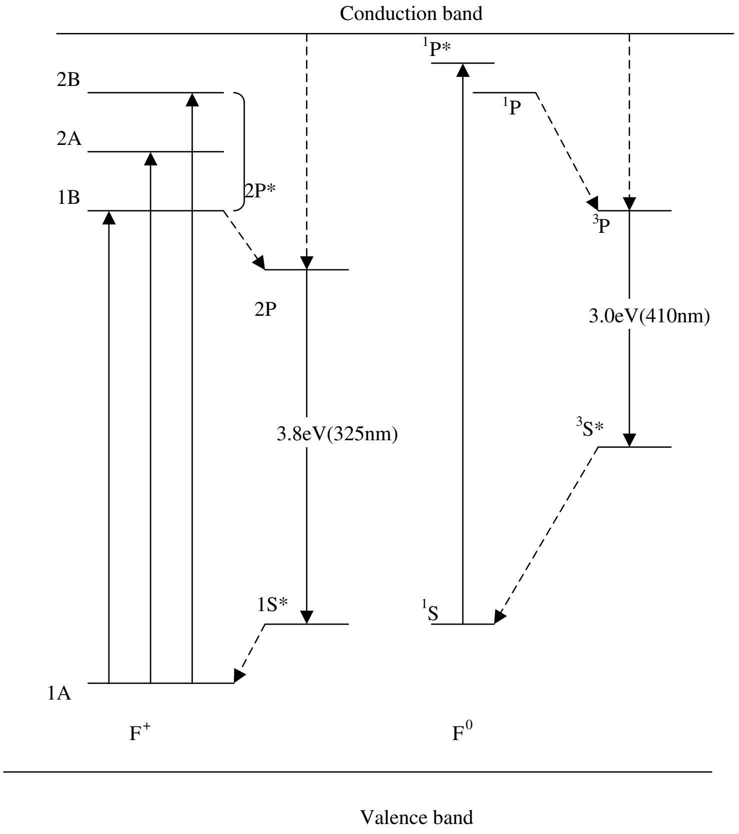

Fig. 6. Flat-band diagram of α-alumina and sapphire summarizing the relative energy positions of F-type centers [7].

fact, each luminescence intensity is rather constant in the lower temperature region, indicating very low activation energy of reactions (1) and (4). The others of the pre-exponential terms and the generation rates are treated to be independent as much as possible in order to make the differences clear. With these assumptions, Eqs. (6) and (7) are thus rewritten as

$$I_{330} = \frac{\left(\frac{C_{F^+} g_{F^+}}{A_1}\right)}{1 + \left(\frac{A_2}{A_1}\right)\cdot \exp\left(-\frac{E_2}{RT}\right) + \left(\frac{A_3}{A_1}\right)\cdot \exp\left(-\frac{E_3}{RT}\right)} = \frac{g'_{F^+}}{1 + k'_2 + k'_3}, \qquad (10)$$

$$I_{420} = \frac{\left(\frac{C_{F^0} g_{F^0}}{A_4}\right) + \left(\frac{C_{F^0} A_1}{C_{F^+} A_4}\right)\cdot \frac{\left(\frac{C_{F^+} g_{F^+}}{A_1}\right)\cdot\left(\frac{A_3}{A_1}\right)\cdot \exp\left(-\frac{E_3}{RT}\right)}{1+\left(\frac{A_2}{A_1}\right)\cdot\exp\left(-\frac{E_2}{RT}\right)+\left(\frac{A_3}{A_1}\right)\cdot\exp\left(-\frac{E_3}{RT}\right)}}{1 + \left(\frac{A_5}{A_4}\right)\cdot \exp\left(-\frac{E_5}{RT}\right)} = \frac{g'_{F^0} + C' \cdot \frac{g'_{F^+}\cdot k'_3}{1+k'_2+k'_3}}{1 + k'_5}, \qquad (11)$$

The measured luminescence intensity data were fitted to Eqs. (10) and (11) by least-squares method, and the parameter values were obtained as summarized in Table 2. As shown in Figs. 3(a), (b) and 4(a) and (b), the agreements are satisfactorily good in all the cases.

The activation energy values are obtained to be 78.8, 141.9, 37.2 kJ/mol for E_2, E_3, and E_5, respectively, in the case of α-alumina while those are 84.5 kJ/mol, 205.0 kJ/mol, 80.5 kJ/mol in sapphire. In view of the reaction scheme, these values are considered to correspond to those of the diffusion of the O_2^- and O_2. In the present analysis, however, it is reminded that the activation energy values for reactions (1) and (4) are assumed to be zero, and the obtained E_2, E_3, and E_5 values may be of approximate ones. In spite of this limitation, it seems that the obtained E_2, E_3, and E_5 values are higher in sapphire than those in α-alumina, reflecting some differences in both materials. As for the pre-exponential term A_i, it is noted that the A_2/A_1, A_3/A_1 and A_5/A_4 values with He^+ irradiation are higher than those with H^+ irradiation in every case. This may be due to the difference in specific ionization between both projectile ions. The specific ionization of He^+ is much higher than that of H^+, and all the reactions of irradiation defects

Table 2
Optimum parameter values obtained from the analysis of in situ luminescence measurement data

Specimen	Projectile	$k'_2 = A_2/A_1 \exp[-E_2/RT]$		$k'_3 = A_3/A_1 \exp[-E_3/RT]$		$g'_{F^+} = \frac{C_{F^+} g_{F^+}}{A_1}$ (s^{-1})
		A_2/A_1	E_2 (kJ/mol)	A_3/A_1	E_3 (kJ/mol)	
α-Al_2O_3	H^+	2.3×10^7	78.8	2.7×10^9	141.9	5.3×10^3
	He^+	6.4×10^7	(78.8)[a]	2.6×10^{11}	(141.9)[a]	3.9×10^3
Sapphire	H^+	9.1×10^7	84.5	9.3×10^{15}	205.0	5.6×10^3
	He^+	9.3×10^8	(84.5)[a]	2.1×10^{17}	(205.0)[a]	6.5×10^3
		$k'_5 = A_5/A_4 \exp[-E_5/RT]$		$C' = \frac{C_{F^0} A_1}{C_{F^+} A_4}$		$g'_{F^0} = \frac{C_{F^0} g_{F^0}}{A_4}$ (s^{-1})
		A_5/A_4	E_5 (kJ/mol)			
α-Al_2O_3	H^+	2.3×10^4	37.2	2.7×10^0		2.2×10^3
	He^+	3.7×10^4	(37.2)[a]	3.0×10^0		7.1×10^2
Sapphire	H^+	2.4×10^9	80.5	3.5×10^2		4.7×10^3
	He^+	4.2×10^9	(80.5)[a]	6.3×10^1		8.8×10^2

[a] Assumed to be the same for the same specimen.

are enhanced with He^+ irradiation. An interesting difference is also found in the g'_{F^+} and g'_{F^0} values. Different g'_{F^0} values are obtained with different projectile ions while no apparent difference is obtained for the g'_{F^+}. By taking into account the lifetimes of $F^+(2P)$ and $F^0(^3P)$, an explanation may be given as follows. In the case of F^+ (2P), the lifetime in the order of 10^{-9} s [10,11] is too short to be involved in the defect reactions especially at lower temperatures. On the other hand, the lifetime of the $F^0(^3P)$ in the triplet state is considerably longer (25 ms [11]), and the defect reactions are likely to affect and reduce the luminescence yield even at lower temperatures, as observed in the present study.

4. Conclusions

In order to know the production behavior of irradiation defects in α-alumina and sapphire, the temperature dependence of the luminescence intensity was studied by an in situ luminescence technique. The temperature dependence of the 330 nm luminescence was well explained by considering the production of the F^+ centers with some competing reactions. In the case of the 420 nm luminescence of the F^0, its non-monotonic temperature dependence was also interpreted by considering a number of competing reactions including the production of the F^0 at higher temperatures. Some of the defect centers were thus confirmed to be formed and to play a critical role in the reaction scheme at high temperatures, at which these ceramic materials would be used.

Acknowledgements

The authors wish to thank Mr K. Yoshida, Kyoto University, for his kind experimental supports.

References

[1] H. Moriyama, S. Tanaka, K. Noda, J. Nucl. Mater. 258–263 (1998) 587.

[2] Y. Asaoka, H. Moriyama, K. Iwasaki, K. Moritani, Y. Ito, J. Nucl. Mater. 183 (1991) 174.

[3] Y. Asaoka, H. Moriyama, Y. Ito, Fusion Technol. 21 (1992) 1944.

[4] Y. Asaoka, H. Moriyama, K. Iwasaki, K. Moritani, Y. Ito, J. Nucl. Mater. 191–194 (1992) 268.

[5] H. Moriyama, T. Nagae, K. Moritani, Y. Ito, Nucl. Instrum. and Meth. B 91 (1994) 317.

[6] K. Moritani, S. Tanaka, H. Moriyama, J. Nucl. Mater. 281 (2000) 106.

[7] B.D. Evans, J. Nucl. Mater. 219 (1995) 202.

[8] A. Al Ghamdi, P.D. Townsend, Nucl. Instrum. and Meth. B 46 (1990) 133.

[9] A. Morono, E.R. Hodgson, J. Nucl. Mater. 249 (1997) 128.

[10] S.Y. La, R.H. Bartram, R.T. Cox, J. Phys. Chem. Solids 34 (1973) 1079.

[11] R. Toshima, H. Miyamaru, J. Asahara, T. Murasawa, A. Takahashi, J. Nucl. Sci. Technol. 39 (2002) 15.